

Raman Crosstalk Suppression in NG-PON2 Using Optimized Spectral Shaping

*Original*

Raman Crosstalk Suppression in NG-PON2 Using Optimized Spectral Shaping / Cantono, Mattia; Curri, Vittorio; Gaudino, Roberto. - In: JOURNAL OF LIGHTWAVE TECHNOLOGY. - ISSN 0733-8724. - 33:24(2015), pp. 5284-5292. [10.1109/JLT.2015.2501058]

*Availability:*

This version is available at: 11583/2638033 since: 2016-03-21T16:08:21Z

*Publisher:*

IEEE

*Published*

DOI:10.1109/JLT.2015.2501058

*Terms of use:*

This article is made available under terms and conditions as specified in the corresponding bibliographic description in the repository

*Publisher copyright*

(Article begins on next page)

# Raman Crosstalk Suppression in NG-PON2 using Optimized Spectral Shaping

Mattia Cantono, *Student Member, IEEE*, Vittorio Curri, *Member, IEEE*, and Roberto Gaudino, *Senior Member, IEEE*,

**Abstract**—In this paper we present an innovative proposal to mitigate the effect of Raman crosstalk in the interaction between NG-PON2 TWDM-PON channels and legacy RF-Video by electrical spectral shaping on the TWDM NRZ data stream obtained through electrical FIR filtering. We find an analytical and closed form solution on FIR filter taps that, for a given target spectral shaping, gives the absolute minimum amount of inter-symbol interference on the TWDM data. Then we propose techniques to implement these FIR filters with reasonable system complexity. We found that our proposed technique is applicable to all classes (up to E2 PON, +11dBm transmitted downstream power) with less than 0.5 dB power penalty on TWDM channels even in the worst case scenario of RF-video still based on analog channels on the lower part of the spectrum.

**Index Terms**—Optical fiber communication, passive optical networks, NGPON2

## I. INTRODUCTION

**F**SAN and ITU-T are currently finalizing details of the physical layer standard for Next Generation Passive Optical Networks (NG-PON2, as specified in ITU-T 989 Recommendation [1]). In this paper we investigate a problem that arose during the definition of this standard: in a full coexistence scenario (Fig. 1) the  $N_{\text{TWDM}}$  optical signals for the new Time and Wavelength Division Multiplexed PON (TWDM-PON) channels may non-linearly interact with the lower wavelength legacy channels (GPON, RF-Video and XG-PON) due to nonlinear Raman effects along the PON feeder fiber for the downstream direction. This has two main consequences: (i) a power transfer takes place between the lower wavelengths, for example GPON and upper TWDM-PON wavelengths, since lower  $\lambda$  channels act as Raman pumps for TWDM-PON signals; (ii) nonlinear optical crosstalk takes place between TWDM-PON signals and legacy PON channels, in particular video overlay channel (RF-Video). (i) has been widely studied in the last two years, especially in order to evaluate additional penalty that legacy systems such as GPON may suffer [2]–[4]. (ii) is mostly relevant for RF-Video, made of a series of electrically modulated subcarriers in the radio frequency (RF) spectrum (from 55 MHz to 1 GHz), using either analog or digital techniques. Legacy analog video channels are extremely sensitive even to small impairments [5]. SRS-induced RF crosstalk causes a degradation in the carrier-to-noise ratio (CNR) of RF-Video subcarriers [5]–[8].

In this paper, starting from previous literature [5], [6] we study the technique of using electrical spectrum shaping on

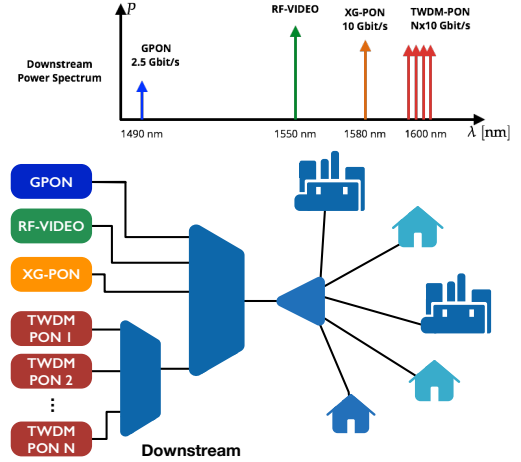


Figure 1. TWDM-PON full coexistence scenario. Downstream spectrum is depicted.

TWDM-PON signals to reduce SRS crosstalk. In particular, we propose an optimal crosstalk suppression strategy based on digital filtering through a Finite Impulse Response (FIR) filter of the TWDM-PON NRZ data that, for a given target spectral reshaping, minimizes intersymbol interference (ISI) on the TWDM-PON signals. Previous proposals to solve the SRS crosstalk over RF-Video were based, for example in [8] on simple electrical RF-filtering and in [9] on dicode coding. However both solutions have some drawbacks. Simple electrical RF-filtering of TWDM-PON signals through notch filters [8] does not allow a well-tuned suppression of SRS crosstalk, while line coding techniques [9] either introduce an overhead to the bitrate (for instance using 8B10B) or a great increase in required electrical bandwidth (for instance for dicode coding). The solution proposed in this paper does not require any overhead on the bit rate of the TWDM-PON signals.

The paper is organized as follows: Section II is devoted to review the physics of SRS crosstalk and to derive the amount of spectral reshaping needed on TWDM-PON in order to obtain a controlled suppression of this effect. In Section III the design of the optimal FIR filter is described while Section IV deals with the system penalty on TWDM-PON signals due to the filtering operation. Finally, some possible practical and cost-effective implementations of the proposed filter are discussed and conclusions are given.

The main novelties of this paper can be summarized as follows:

M. Cantono, R. Gaudino and V. Curri are with Dipartimento di Elettronica e Telecomunicazioni, Politecnico di Torino, Italy (email: mattia.cantono@polito.it)

- the development of a technique that can generate the minimum possible amount of ISI for an arbitrary target spectral masks on the TWDM NRZ data stream
- the closed form evaluation of the resulting ISI and the following definition of PON full coexistence scenarios where this technique can be applied with a given maximum level penalty on TWDM (e.g. 0.5 dB)
- an approximation of the resulting optimal FIR filter to a slightly suboptimal version that still greatly reduces the filter length and implementation complexity.

## II. SRS INDUCED CROSSTALK

In this section we develop an analytical framework for SRS crosstalk following the theory developed in [5], [6], where it is modeled as an additional source of relative intensity noise (RIN) spuriously imposed on the RF-Video channels by the TWDM-PON NRZ modulation. The resulting CNR of the  $i$ -th RF-Video analog subcarrier at the receiver can be written, in linear units as:

$$\text{CNR}_i = \frac{\frac{1}{2}m_i^2 P_i^2}{B_{e,i}(i_{th}^2 + i_{sh}^2) + B_{e,i}[\text{RIN}(f_i) + \text{RIN}_{\text{SRS}}(f_i)] P_i^2} \quad (1)$$

where  $\text{RIN}_{\text{SRS}}(f_i)$  is the RIN around the electrical frequency  $f_i$  originated from SRS effects,  $m_i$  is the  $i$ -video channel modulation index (usually set to 3.5%),  $P_i$  is its received optical power,  $B_{e,i}$  is the electrical bandwidth of the video channel receiver filter (usually 4.2 MHz for the analog video channel that are more critical in the considered scenario),  $i_{th}$  is the equivalent thermal noise spectral density of the receiver,  $i_{sh}$  is the shot noise characteristic and  $\text{RIN}(f_i)$  is the RIN from other sources different from SRS effects. Neglecting these last two terms, we can simplify Eq. (1) to:

$$\text{CNR}_i = \frac{1}{\frac{1}{\text{CNR}_{th,i}} + \frac{1}{\text{CNR}_{\text{SRS},i}}} \quad (2)$$

where  $\text{CNR}_{th,i}$  is the reference design CNR, that does not consider additional impairments due to SRS, and it is given by

$$\text{CNR}_{th,i} = \frac{\frac{1}{2}m_i^2 P_i^2}{B_{e,i}i_{th}^2}. \quad (3)$$

$\text{CNR}_{th,i}$ , for analog RF-Video channels, is usually set around 50 dB as prescribed both by ITU-T [10] and FCC [11] but the minimum value of  $\text{CNR}_i$  for which analog channels are considered to be operative is instead 7 dB lower than the target design value  $\text{CNR}_{th,i}$ , i.e. 43 dB as suggested by [10] and FCC [11]. The term  $\text{CNR}_{\text{SRS},i}$  includes instead all additional SRS induced impairments and it is given by

$$\text{CNR}_{\text{SRS},i} = \frac{\frac{1}{2}m_i^2}{B_{e,i}\text{RIN}_{\text{SRS}}(f_i)} \quad (4)$$

Considering the theory developed in [12] and in [5], it is possible to write  $\text{RIN}_{\text{SRS}}(f_i) = \text{RIN}_{\text{TWDM}}(f_i) \cdot G_{\text{SRS}}(f_i)$ , i.e. as the product of the RIN of the "input signal", that in this case is the non-return-to-zero (NRZ) modulation of a single TWDM-PON channel  $\text{RIN}_{\text{TWDM}}(f_i)$  and a SRS RIN transfer

function,  $G_{\text{SRS}}(f_i)$ . In particular,  $G_{\text{SRS}}(f_i)$  can be written as the product of three terms:

$$G_{\text{SRS}}(f_i) = G_{\text{RIN0}} \cdot G_{\text{LP}}(f_i) \cdot G_{\text{RIP}}(f_i) \quad (5)$$

where  $G_{\text{RIN0}} = C_r N_{\text{TWDM}} P_{\text{TWDM}}$  is a frequency-independent term that directly depends on the number of TWDM-PON channels  $N_{\text{TWDM}}$  and their average power  $P_{\text{TWDM}}$  and the polarization averaged Raman efficiency  $C_r$  [1/mW/km]. The first frequency-dependent term in Eq.(5) is  $G_{\text{LP}}(f_i) = \alpha^{-2}/(1+f_i^2/f_c^2)$ , which is the equivalent of a single pole low-pass term with corner frequency  $f_c = (2\pi D\Delta\lambda)/\alpha$ , where  $D$  is the fiber chromatic dispersion coefficient [ps/nm/km],  $\Delta\lambda$  is the optical spectral separation between the RF-Video channels and the TWDM-PON channels measured in nm,  $\alpha$  is the fiber loss coefficient in 1/km. For standard single mode fiber (SMF) ( $D = 16.7$  ps/nm/km,  $\alpha_{\text{dB}} = 0.2$  dB/km), and  $\Delta\lambda = 50$  nm, as in our case,  $f_c \approx 9$  MHz. The second frequency-dependent term in Eq.(5) is  $G_{\text{RIP}}(f_i) = 1 - 2\exp(-\alpha L)\cos(2\pi D\Delta\lambda L f_i) + \exp(-2\alpha L)$ , that is a frequency-oscillating term that becomes negligible for fiber lengths larger than the fiber effective length [12] (i.e. around  $L=22$  km). It should be noted that due to the low pass characteristic of  $G_{\text{SRS}}(f_i)$ , the RF-Video subcarriers that are impaired the most by SRS crosstalk are the lower frequency ones (i.e. around 55 MHz), while for higher frequency the chromatic dispersion induced walk-off effects progressively reduce the SRS impairments.

Considering that in our scenario the  $N_{\text{TWDM}}$  TWDM-PON channels are made of scrambled NRZ data streams without any line coding, the term  $\text{RIN}_{\text{TWDM}}(f_i)$  can be written as [5] the power spectral density of a random 2-PAM modulation stream, i.e. as:

$$\text{RIN}_{\text{TWDM}}(f_i) \approx 2S_c(f_i) = 2S_c^{\text{NRZ}}(f_i) = \frac{2}{R_b} \frac{\sin^2\left(\frac{\pi f_i}{R_b}\right)}{\left(\frac{\pi f_i}{R_b}\right)^2} \quad (6)$$

where  $S_c^{\text{NRZ}}(f_i)$  is the power spectral density of scrambled NRZ data, and  $R_b$  is the bit rate, i.e. 10 Gbps. Here we have assumed rectangular NRZ pulses in the time domain to have a simple expression. However it should be noted that this assumption is not relevant for other more realistic NRZ pulses since only the lower frequency components of  $S_c^{\text{NRZ}}(f_i)$  are significant due to the aforementioned low-pass characteristic of  $G_{\text{LP}}(f_i)$ , and these are almost independent on the NRZ pulse shape. In fact, it turns out in our numerical evaluations that in all cases of interest the only relevant term is  $\text{RIN}_{\text{TWDM}}(0) = \frac{2}{R_b}$ .

Using the previous equations, we can evaluate Eq. (2) for each RF-Video subcarrier in order to verify whether their CNR is greater or equal than the minimum CNR required for correct operation, which in both [10] and [11] it is set to  $\text{CNR}_{\text{min}}^{\text{dB}} = 43$  dB. Now our goal is to find the maximum tolerable  $\text{RIN}_{\text{SRS}}(f)$  still ensuring a CNR greater than the minimum required. Considering that without SRS effects the analog channels are designed to have a target  $\text{CNR}_{th}^{\text{dB}} = 50$  dB, one can derive the maximum acceptable SRS induced RIN for the  $i$ -th RF-Video subcarrier, as the term that brings down the

CNR from  $\text{CNR}_{th}^{\text{dB}} = 50$  to  $\text{CNR}_{\min}^{\text{dB}} = 43$  dB, obtaining the following condition (in which all terms should be expressed in linear units):

$$\text{RIN}_{\text{SRS}}(f_i) \leq \frac{\text{CNR}_{th,i} - \text{CNR}_{\min}}{\text{CNR}_{th,i} \text{CNR}_{\min}} \frac{m_i^2}{2B_{e,i}} = K \quad (7)$$

It can be noted that the right-hand side of the previous equation is independent from  $f_i$ , therefore it represents an upper bound for all RF-Video channels. Moreover, considering Eq. (5) and omitting the term  $G_{\text{RIP}}(f_i)$  in order to obtain a result that is independent on the link length and that considers the worst case scenario, we can rewrite the last equation introducing useful dB units as:

$$\text{RIN}_{\text{TWDM}}^{\text{dB}}(f_i) + G_{\text{RIN0}}^{\text{dB}} + G_{\text{LP}}^{\text{dB}}(f_i) \leq K^{\text{dB}} \quad (8)$$

Now we can introduce the main idea of our paper. Referring to Eq. (8) and Eq. (6), one can derive the amount of spectral shaping that one needs to apply to scrambled NRZ to reduce the impact of TWDM-PON channels on RF-Video according to the condition expressed by Eq. (8), that ensures a CNR greater or equal than minimum required for each RF-Video subcarrier. In other terms, we assume that the power spectral density (PSD) of a single TWDM-PON channel is not the one expressed with Eq. (6) but it is modified by an appropriate electrical filter to:

$$S_c^{\text{dB}}(f_i) = 10 \log_{10}[S_c^{\text{NRZ}}(f_i)] + \Delta S^{\text{dB}}(f_i). \quad (9)$$

where the term  $\Delta S^{\text{dB}}(f_i)$  is the modulus squared (in dB) of the applied filter, and it represents the amount of spectral shaping to be applied on each TWDM-PON channel to allow correct operations of RF-Video channel at frequency  $f_i$ . Plugging this last equation back into Eq. (8) we get:

$$\Delta S^{\text{dB}}(f_i) \leq K^{\text{dB}} - 10 \log_{10}[2S_c^{\text{NRZ}}(f_i)] - G_{\text{RIN0}}^{\text{dB}} - G_{\text{LP}}^{\text{dB}}(f_i). \quad (10)$$

This is a first fundamental result of our paper: given the main system parameters, such as  $P_{\text{TWDM}}$  and  $N_{\text{TWDM}}$  and the link characteristics, Eq. (10) gives a general formulation of the spectral shaping to be applied on the (uncoded) TWDM-PON channels to keep legacy RF-video in-service in case of full co-existence. In particular, for a channel at frequency  $f_i$ , if  $\Delta S^{\text{dB}}(f_i)$  is found to be negative, the PSD of each TWDM-PON channel must be reduced of at least  $|\Delta S^{\text{dB}}(f_i)|$  dB. If positive, no PSD modifications should be applied.

We performed numerical evaluations of Eq. (10) at the frequencies of interests (i.e., from 55 MHz to 1 GHz where the video subcarriers are placed [11]), considering either 4 or 8 TWDM-PON channels, and the three different transmitted optical powers proposed in the last TWDM-PON standard [1] ( $P_{\text{TWDM}} = 7, 9, 11$  dBm per downstream channel, as envisioned by the ITU-T G.989.2), while standard SMF was considered for transmission ( $\alpha_{\text{dB}} = 0.2$  dB/km;  $D = 16.7$  ps/nm/km). We assumed the fiber length  $L$  to be larger than the fiber effective length (i.e. around 22 km) so as to being able to compute Eq. (10) independently on  $L$  and in a worst-case condition (for lower lengths SRS effects would be obviously lower). The analysis was performed considering both the worst and best-case scenarios in terms of relative polarization for

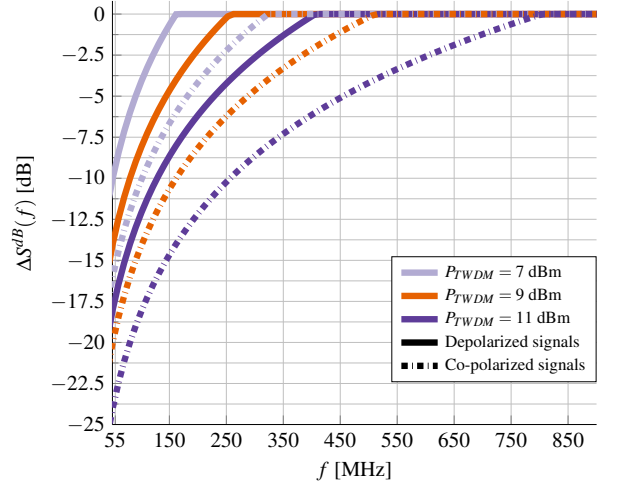


Figure 2. Required spectral shaping  $\Delta S^{\text{dB}}(f)$  for  $N_{\text{TWDM}} = 8$ , and three different  $P_{\text{TWDM}}$ . The fiber characteristics are  $\alpha_{\text{dB}} = 0.2$  dB/km;  $D = 16.7$  ps/nm/km.

TWDM-PON and RF-Video channels and consequent SRS efficiency [4]. We defined the (polarization) worst-case as the one where all channels are perfectly co-polarized along all the fiber length. This is a worst-case bound for aligned launch and very low Polarization Mode Dispersion (PMD) fibers, which is very unlikely in access networks where fiber with reasonable PMD values (usually  $\leq 0.04$  ps/sqrt(km)) are usually installed [4], thus polarization alignment between 50-nm spaced optical signals is lost after few km of propagation, as discussed in [4]. On the contrary, for normal to high-PMD values (or in case depolarization strategies on TWDM-PON channels at the transmitter [4]), the SRS efficiency is one-half with respect to the worst-case scenario (in dB) [13]. This case is by far the most likely in PON, where the PMD coefficients and the lengths of the installed fiber are sufficiently large to guarantee an intrinsic depolarization "scrambling" along the fiber length on 50-nm spaced optical signals, as it happens for RF-Video and TWDM-PON in downstream transmission.

As first example of our analysis, Fig. 2 shows the amount of spectral shaping required for different system parameters (and  $N_{\text{TWDM}} = 8$ ). As anticipated, spectral shaping is needed at lower frequency up to a given frequency which depends on system parameters and whose amount increases for increasing average TWDM-PON power per channel. In fact, as  $P_{\text{TWDM}}$  increases, more and more RF-Video channels are impaired by SRS, and consequently the bandwidth over which the spectral shaping must be effectively applied enlarges. For the worst case scenario, i.e.,  $P_{\text{TWDM}} = 11$  dBm, and copolarized signals, this bandwidth is even beyond 800 MHz.

### III. DESIGN OF OPTIMAL FIR FILTERS

While in the previous Section we defined the amount of spectral shaping required and expressed it through the fundamental Eq. (10), in this section we focus on the fact that any filtering effect on the TWDM-PON NRZ stream will create a penalty on these channels [14], due to the generation of Inter Symbol Interference (ISI) on the NRZ data. It is

intuitive, but this will be demonstrated later on, that the more pronounced is the "spectral notch" that should be created on the NRZ spectrum, the higher will be the resulting penalty due to ISI. In this Section, we thus rigorously derive how to design an optimized FIR filter that implements spectral shaping such as those shown in Fig. 2 and at the same time generates the *minimum* possible amount of ISI on the NRZ stream.

We started by observing that, as highlighted in [15], the power spectral density of a digital signal  $y$  with symbols that are time-correlated (due either to filtering or to line coding) is given by:

$$S_y(f) = \frac{1}{T} |G(f)|^2 \sum_{k=-\infty}^{+\infty} R_y(k) e^{-j2\pi k f T} \quad (11)$$

$$= \frac{1}{T} |G(f)|^2 S_x(f) \quad (12)$$

where the term  $G(f)$  is the Fourier transform of the basic modulation pulse, and  $R_y(k)$  is the discrete autocorrelation function of the information bit sequence  $y$ . Referring to our specific scenario, the term  $G(f)$  can be considered as constant over the bandwidth of interest, since the required spectral shaping in Fig. 2 does not go above 800 MHz even for the highest power levels  $P_{\text{TWDM}}=11$  dBm, while the downstream bit rate in TDWD-PON is 10 Gbps.

The term  $S_y(f) = \sum_{k=-\infty}^{+\infty} R_y(k) e^{-j2\pi k f T}$  depends on the correlation properties that the FIR filter adds to the independent scrambled input TWDM-PON bits. We thus need to develop a filter such that the squared modulus of its transfer function  $|H(f)|^2$  is equal to  $\Delta S^{\text{dB}}(f)$  for  $f \in [55, f_u]$  MHz, where  $f_u$  is the frequency at which  $\Delta S^{\text{dB}}(f)$  goes to zero. Provided that these constraints are respected we can allow  $|H(f)|^2$  to vary freely outside of the interval  $[55 \text{ MHz}, f_u]$ . At the same time, we want to minimize the resulting ISI. Having in mind a simplified system implementation - as it will be discussed in more details in Section V - we focus on the design of a digital filter operating at one sample per bit on the input uncoded data stream. Since the spectral mask should be respected down to the lowest video channel electrical frequency (around 55 MHz) we should synthesize the FIR filter to have a sufficiently fine frequency grid (of the order of  $\Delta f \leq 10$  MHz). Consequently, since we want to run the filter at 10 Gsample/s (for TWDM-PON at 10 Gbps) we need to consider a filter of at least  $N = 1000$  taps since the filter frequency grid will be given by  $10 \text{ Gsample/s}/N$ . To summarize, we have to design a filter subject to the fact that  $N_c$  frequency points out of  $N$  are defined by  $\Delta S^{\text{dB}}(f)$  and generating the minimum possible ISI.

We can generally write that the FIR filter output sample  $y_n$  is given by:

$$y_n = h_n x_n + \sum_{\substack{i=0 \\ i \neq n}}^{N-1} h_i x_{n-i} \quad (13)$$

where  $x_n$  is the sequence of uncoded input bits. Thus, the  $n$ -th output sample is given by the summation of the useful contribution for the bit in the  $n$ -th position, plus the ISI term depending on all other transmitted bits. Neglecting the irrelevant DC-component in the uncoded NRZ stream, we can

normalize the input bits to  $x_n = \{+1, -1\}$  and then quantify ISI by referring to the so-called ISI root mean square distortion  $D_{\text{RMS}}$  [15], i.e.:

$$D_{\text{RMS}} = \sqrt{\frac{\sum_{i \neq n} |h_i|^2}{|h_n|^2}} \quad (14)$$

To further simplify the expression of  $D_{\text{RMS}}$ , without loss of generality thanks to the stationarity of the resulting discrete random processes, we can refer to the output sample at position  $n = 0$  and normalize  $h_0 = 1$ , thus having:

$$D_{\text{RMS}}^2 = \sum_{i=0}^{N-1} |h_i|^2 - 1 \quad (15)$$

Since the spectral mask is expressed in the frequency domain, we exploit the Parseval equality to rewrite this last equation, knowing that the transfer function of a FIR filter is the discrete Fourier transform of the impulse response, obtaining:

$$D_{\text{RMS}}^2 = \frac{1}{N} \sum_{i=0}^{N-1} |H_i|^2 - 1 \quad (16)$$

which is our "cost function" to be minimized in order to minimize ISI. We now observe that the constraint set by  $\Delta S^{\text{dB}}(f)$  is not strictly given over the full spectrum, but only in a frequency range of the order shown in Fig. 2. Let's indicate as  $F_f$  the spectral points that fall in this frequency range. For instance, assuming a FIR filter with  $N = 1000$  taps running at 10 Gsample/s (thus having a spectral resolution equal to 10 MHz) and a SRS spectral mask defined inside the range  $[55 \text{ MHz}, f_u]$  with  $f_u=750$  MHz, i.e. over approximately 700 MHz, the "SRS-constrained" spectral window contains  $F_f=70$  points, while all other points are constraint-free in terms of SRS reduction.

Thanks to all these observations, we can ultimately express our constrained minimization problem as follows:

$$\text{minimize } \frac{1}{N} \sum_{H_i \in F_f} |H_i|^2 \quad (17)$$

$$\text{subject to } h_0 = \frac{1}{N} \sum_{i=0}^{N-1} H_i = 1 \quad (18)$$

$$|H_i|^2 = \Delta S^{\text{dB}}(f_i) \text{ for } f \in [55 \text{ MHz}, f_u] \quad (19)$$

This formulation can be further simplified by following the details given in Appendix A, where it is also shown that it can be safely assumed  $H_i$  to be a real number. The final formulation of the problem is therefore:

$$\text{minimize } \frac{1}{N} \sum_{H_i \in F_f} |H_i|^2 \quad (20)$$

$$\text{subject to } \sum_{H_i \in F_f} H_i = b \quad (21)$$

where  $b$  is constant given by

$$b = N - \sum_{H_i \in F_c} H_i = N - \sum_{i \in F_c} \sqrt{\Delta S^{\text{dB}}(f_i)} \quad (22)$$

We have therefore defined the design of an optimal FIR filter as a classic minimization problem. In Appendix A, a geometrical

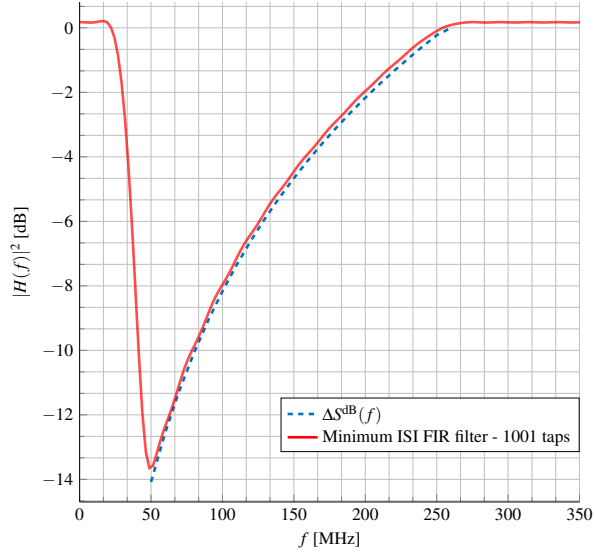


Figure 3. Comparison between a target  $\Delta S^{\text{dB}}(f)$  and the  $|H(f)|^2$  resulting from the minimum ISI FIR filter design. Parameters:  $N_{\text{TWDM}} = 8$ ,  $P_{\text{TWDM}} = 9$  dBm, depolarized signals,  $\alpha_{\text{dB}} = 0.2$  dB/km;  $D = 16.7$  ps/nm/km.

interpretation to this minimization problem given by Eq. (20) and Eq. (21) is shown and, surprisingly, it is possible to obtain a closed-form solution given by:

$$H_i = \frac{b}{N_f} \quad \text{for } H_i \in F_f \quad (23)$$

where  $N_f = N - N_c$  is the number of unconstrained points of the FIR transfer function, while the constrained spectral points should satisfy the SRS spectral mask  $|H_i|^2 = \Delta S^{\text{dB}}(f)$ . We can summarize the result in a very simple way: the optimal transfer function is constant outside the bandwidth  $f \in [55 \text{ MHz}, f_u]$ , while it falls exactly on the spectral mask for the constrained points.

As an important observation, the resulting transfer function has a strong similarity with the triangular-shaped filter proposed in [14] for the same problem. The novelty of our work compared to [14] is anyway two-fold: (i) we have obtained an expression for the absolute optimal condition (in the ISI sense previously introduced) and (ii) we provided a rigorous way to synthesize the resulting filter.

Having now defined the desired frequency response behaviour for all  $N$  points of the FIR filter transfer function, the FIR taps can be computed by using existing synthesis algorithm such as the frequency sampling method [16] that computes the FIR taps coefficient through appropriate interpolation, inverse discrete Fourier transform (DFT) and windowing. This method provides better results with respect to directly computing inverse DFT of the target transfer function since it allows to obtain smoother transfer functions at the expense of small differences (fractions of dB) with respect to the desired spectral mask, and slightly worse ISI.

As an example of application of our results, Fig. 3 depicts the desired spectral mask and the resulting transfer function for a FIR filter designed to suppress SRS-induced crosstalk for a typical TWDM-PON scenario with parameters  $N_{\text{TWDM}} = 8$ ,  $P_{\text{TWDM}} = 9$  dBm, and RF-Video and TWDM-PON channels

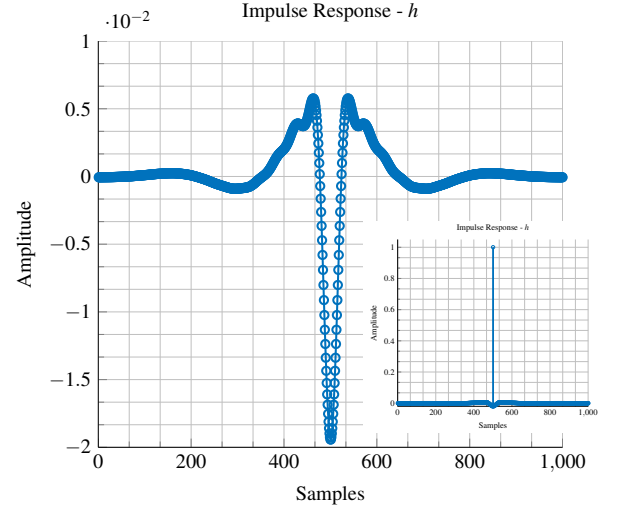


Figure 4. Impulse response of the minimum ISI FIR filter ( $N=1001$ , symmetric impulse response), omitting central unity tap.  $N_{\text{TWDM}} = 8$ ,  $P_{\text{TWDM}} = 9$  dBm, depolarized signals. In inset, the full impulse response with the unity tap.

depolarized along the full fiber length (i.e. for typical PMD values). We observe that the resulting FIR filter response in the “constrained” range from 55 MHz to  $f_u$  is at most 0.2 dB larger than the target  $\Delta S^{\text{dB}}(f)$ , a difference that can be considered as negligible in the current scenario.

In the following Fig. 4 we present the resulting FIR impulse response in the time domain, omitting the central sample set to 1, so as to obtain a readable plot on the amplitude axis (the full impulse response is depicted in the inset of Fig. 4)

As it can be noted, the filter taps are (individually) very small compared to the unity central sample and they very slowly oscillate around zero. Anyway, they may generate non-negligible ISI due to their high number. Moreover, the impulse response is symmetric as its phase is linear. All these observations will be the basis for a great simplification in the FIR filter implementation through proper decimation and truncation strategies, as discussed in Section V.

#### IV. SYSTEM PENALTY ON TWDM-PON SIGNALS

In this section, the system penalty caused by the filtering operations on TWDM-PON signals will be discussed in the following 12 different scenarios:

- $N_{\text{TWDM}} = 4$  or  $N_{\text{TWDM}} = 8$
- $P_{\text{TWDM}} \in \{7, 9, 11\}$  dBm
- TWDM-PON channels fully depolarized or completely depolarized with respect to RF-Video channel.

In order to evaluate the resulting ISI for the optimal filter obtained for each case, we implemented a lengthy numerical simulation in which a pseudo-random bit sequence of length  $2^{28} - 1$  was passed through the optimized FIR filters. We used standard semi-analytic techniques for evaluating the resulting BER in the presence of receiver additive Gaussian noise and ISI. Thanks to the extremely long simulated sequence ( $2^{28} \simeq 2.7 \cdot 10^8$  bits), the accuracy of resulting BER estimation turned out to be excellent.



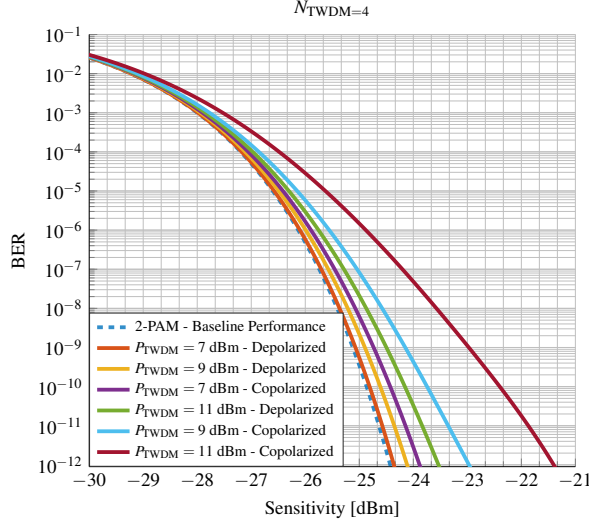


Figure 5. BER vs. receiver sensitivity for different TWDM-PON parameters,  $N_{TWDM} = 4$ . Reference sensitivity value set to  $-28$  dBm at  $BER = 10^{-3}$ .

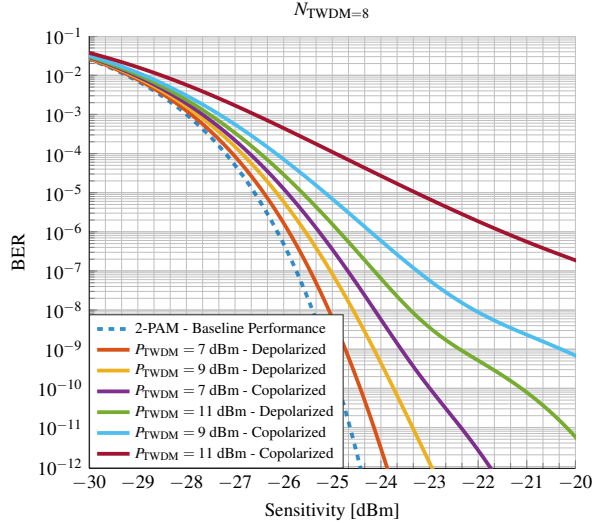


Figure 6. BER vs. receiver sensitivity for different TWDM-PON parameters,  $N_{TWDM} = 8$ . Reference sensitivity value set to  $-28$  dBm at  $BER = 10^{-3}$ .

The results are shown in Fig. 5 and Fig. 6 in terms of BER vs. optical receiver sensitivity, considering a PIN+TIA receiver having a typical back-to-back sensitivity equal to  $-28$  dBm at  $BER=10^{-3}$  (similarly to what is prescribed in [1]).

In Table I we summarized the result of our analysis, reporting the BER penalty with respect to the unfiltered baseline performances computed for BER levels of  $10^{-3}$ , and  $10^{-12}$ . To derive some interesting system considerations, we set the allowable BER penalty at  $10^{-3}$  to be equal to 0.5 dB. Then, it is possible to identify the scenarios for which full SRS Raman Crosstalk is feasible. Table I shows that it is possible to suppress SRS Raman Crosstalk without over-impairing TWDM-PON signals (i.e. with penalty below 0.5 dB), up to the case in which 8 TWDM-PON channels are active with a transmitted power per channel of 11 dBm (under the realistic and quite common depolarized case), which corresponds to the most demanding class (E2) of NG-PON2 standard [1]. In this case, as depicted

Table I  
BER PENALTY AT  $BER=10^{-3}$ , AT  $10^{-12}$ , AND RMS ISI DISTORTION FOR DIFFERENT SYSTEM SCENARIOS

$N_{TWDM}$	$P_{TWDM}$ [dBm]	Copol.	Penalty at $10^{-3}$ [dB]	Penalty at $10^{-12}$ [dB]	$D_{RMS}$
4	7	NO	0.01	0.07	0.019
4	9	NO	0.06	0.31	0.047
8	7	NO	0.10	0.55	0.063
4	11	NO	0.15	0.89	0.080
8	9	NO	0.23	1.46	0.100
8	11	NO	0.47	4.93	0.142
4	7	YES	0.10	0.54	0.063
4	9	YES	0.23	1.46	0.099
8	7	YES	0.33	2.66	0.120
4	11	YES	0.47	4.93	0.142
8	9	YES	0.68	> 5	0.166
8	11	YES	1.40	> 5	0.226

in Fig. 2, the power spectral density of each TWDM-PON channel should be attenuated from 55 MHz to 400 MHz, with a maximum required attenuation of 18 dB at 55 MHz. It can be noted that for the worst case in terms of polarizations (copolarized TWDM-PON and RF-Video signals), complete SRS suppression is feasible only for transmitted power up to 7 dBm per channel. However, as already discussed, this condition is very unlikely.

It is interesting to compare the results of Table I to the one obtained in [8], where Raman crosstalk is mitigated by means of a simpler but sub-optimally shaped RF analog filter. In [8], only a single NRZ signal at 15 dBm is considered, while we consider a more realistic case of several TWDM-PON channels. Still, due to the physics of SRS, a single channel at 15 dBm should generate approximately the same crosstalk as 4 TWDM-PON channels at 9 dBm each, which is one of the entries considered in Table I. With our implementation, the simulated BER penalty is equal to 0.06 dB for depolarized signals, and to 0.23 dB in the copolarized case, whereas in [8] a 1.3 dB penalty is obtained. Thus our implementation, besides being more precise in terms of PSD control for Raman suppression, allows a smaller BER penalty (around 1 dB improvement neglecting any additional experimental impairment) on the filtered TWDM-PON signals.

In addition to BER considerations, Table I also reports the value of the RMS ISI distortion  $D_{RMS}$ , computed by means of Eq. (15), in order to allow a direct comparison with the result found in [14] for perfectly triangular ideal filters, although the ones obtained in this paper are obtained considering a precise spectral shaping given by Eq. (10).

## V. SIMPLIFIED IMPLEMENTATION

The direct implementation of the optimized filters outlined in previous sections would require extremely long FIR filters having a number of taps of the order of 1000. Moreover, the filter output should be generated with digital to analog converters (DAC) that should be operated at very high speeds (10 Gsamples/s). Both requirements may be hard to implement under the extremely tight cost constraints of PON hardware. Focus of this Section is to propose simplified implementations that take advantage on some properties of the FIR filters that come out of the algorithm proposed in the previous section.

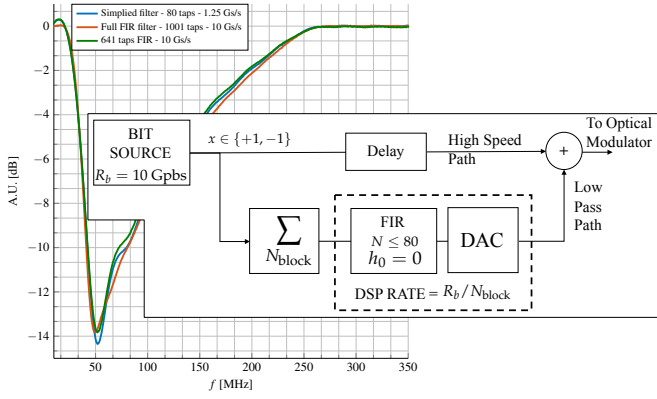


Figure 7. Simulated transfer function obtained from the filtered NRZ stream: comparison between the full rate FIR implementation and two simplified FIR implementations, for  $N_{\text{TWDM}} = 8$ ,  $P_{\text{TWDM}} = 9$  dBm, depolarized signals,  $\alpha_{\text{dB}} = 0.2$  dB/km;  $D = 16.7$  ps/nm/km Inset: block scheme of low rate SRS suppression implementation.

By observing the typical resulting impulse response, such as the one presented in Fig. 4, we note that, apart from the central tap conventionally set to 1:

- 1) all other taps are much smaller than the central one and, overall, they implement a low-pass filtering function whose typical range is below 700 MHz (as previously discussed). Thus it is possible to envision an implementation of the required filtering as shown in the inset of Fig. 7 where we separate a "high speed" path that takes into account the useful central sample i.e., the one whose tap is conventionally set to 1 and that carries the useful NRZ bit (and that would be the typical high speed path of any 10 Gbps optoelectronic transmitter), and a "low-pass" path that takes into account the low-pass nature of the filtering required to implement the SRS spectral mask. Since this second output has a spectrum well-below 700 MHz in all cases of interest, it can be generated with a much slower DAC than the one that would be required with a direct implementation at the full rate (10 Gsamples/s). The high-speed and the low-pass paths should then be summed only on the input electrical port the impulse modulator.
- 2) the impulse response in Fig. 4 is very smooth in the time domain, in the sense that the amplitude variation among adjacent taps is very small. We use this characteristic for a step-wise implementation of the FIR taps. In particular, we tried to approximate a block of  $N_{\text{block}}$  consecutive taps as a single equivalent tap equal to the mean of the  $N_{\text{block}}$  taps, and whose input is not the initial sequence  $x_k = \pm 1$ , but the mean of  $N_{\text{block}}$  consecutive  $x_k$  values. This observation, coupled to the previous one, allows the FIR filter and the following DAC to run at a speed reduced by  $N_{\text{block}}$ , i.e. at  $10/N_{\text{block}}$  Gsamples/s.
- 3) the most external taps in the impulse response goes to zero, which allows for some final truncation of the number of taps without exceedingly high penalty

We studied in detailed these three options, and applied them to the same conditions of Fig. 3 in the previous Section, that is designed to suppress SRS crosstalk caused by 8 depolarized

Table II  
MAXIMUM DIFFERENCE BETWEEN  $|H(f)|^2$  OF TRUNCATED AND DECEMATED FIR AND 1001 TAPS FIR.  $N_{\text{TWDM}} = 8$ ,  $P_{\text{TWDM}} = 9$  dBm, DEPOLARIZED SIGNALS.

		Block Length		
		4	8	16
Truncation	0	$\Delta_L = 0.07$ dB	$\Delta_L = 0.28$ dB	$\Delta_L = 1.07$ dB
	180	$\Delta_L = 0.50$ dB	$\Delta_L = 0.66$ dB	$\Delta_L = 1.27$ dB
	244	$\Delta_L = 0.66$ dB	$\Delta_L = 0.82$ dB	$\Delta_L = 1.43$ dB
	260	$\Delta_L = 0.69$ dB	$\Delta_L = 0.86$ dB	$\Delta_L = 1.50$ dB
	340	$\Delta_L = 3.11$ dB	$\Delta_L = 3.20$ dB	$\Delta_L = 3.53$ dB

TWDM-PON channels at 9 dBm each. As a first example, we evaluate a simplified filter that was obtained by truncating the original 1001 taps filter to 640 taps, and then setting  $N_{\text{block}}=8$ . The resulting simulated transfer function of this simplified FIR was obtained by a very long time domain simulations over a  $2^{28}$  PRBS bit sequence and it is given in Fig. 7 (blue curve), together with the one that would be obtained with the full rate implementation (over 1001, red curve, or 641 taps, green curve).

This simplified filter has a very small difference compared to the full rate one and in particular the maximum difference in the region of interest, i.e. from 55 MHz to  $f_u = 250$  MHz, is  $\Delta_L = 0.66$  dB, which we believe can be acceptable considering that in PON scenario many of the other parameters are given with very large tolerances even in the ITU-T Recommendations. From a practical point of view, the simplified filter would run at  $10 \text{ Gsamples/s} / N_{\text{block}} = 1.25$  Gsamples/s and it would have only 80 taps which can be further reduced to 40 thanks to the symmetry conditions of the impulse response. Overall, this is a great improvement compared to a full rate implementation, since the required DAC would be much simpler (1.25 Gsamples/s DAC are today available in relatively standard CMOS technology, while 10 Gsamples/s DAC requires more sophisticated electronics), and the FIR design would require only 40 real multiplications for each input sample. Finally, we observe that a block processing over  $N_{\text{block}}=8$  bit (1 Byte) would nicely match the typical internal parallelism of high-speed PHY chipsets, therefore, making its adoption much more favorable in real ASICs or FPGAs implementations.

To fully assess the performance of simplified FIR implementations, we evaluate the maximum spectral error in the transfer function  $\Delta_L$  dB in the range of interest for different values of  $N_{\text{block}}$  and truncation, for the same FIR filter designed in Fig. 3, giving the results in Table II.

## VI. CONCLUSIONS

In this paper we proposed the use of FIR filtering on the input uncoded TWDM-PON NRZ stream to obtain a given spectral shaping on the output sequence that would suppress SRS crosstalk in an appropriate way, on the RF-video channel and at the same time minimize the resulting ISI on the TWDM channels. After finding an exact mathematical framework to obtain the closed-form expression of this optimized filter, we found that this solution satisfies a stringent SRS crosstalk suppression mask (even for very demanding analog video channels) with less than 0.5 dB ISI penalty to



all ITU-T TWDM-PON ODN classes (up to E2 PON, +11dBm transmitted downstream power per TWDM-PON channel). We then proposed practical FIR implementation at a reduced rate, finding that in most significant situations a 40x2 taps symmetrical FIR filter can be used with minimal inaccuracy on the resulting spectral mask.

We believe that this paper can be of interest in two areas: (i) within the standardization process for TWDM-PON [1], where the idea of spectral shaping is only mentioned without the actual implementation details; (ii) in any optical transmission situation impaired by Raman crosstalk.

## APPENDIX A

### REAL VALUED SOLUTION TO ISI MINIMIZATION PROBLEM

In this section, a geometrical interpretation to the constrained minimization problem described by Eq. (17), (18), (19) is given. In particular we are looking for the minimization of the square of the root mean square ISI (cf. Eq. (16)), i.e. a quadratic form. This quadratic form can be seen as a convex hyperparaboloid, with absolute minimum in the origin of the plane with  $N_f$  dimensions, where  $N_f$  is the number of unconstrained points of the transfer function. On the other hand, the constraints given by Eq. (18) and (19) represent a hyperplane in a space with  $N_f$  dimensions. Therefore, the minimization problem is equivalent to looking for the minimum point of intersection between a hyperparaboloid and a hyperplane. This problem has a very simple visualization by considering two dimensions only i.e., with  $N_f = 2$  (cf. Fig. 8). In this case, we need to find the circumference that is tangent to a line whose equation is  $H_1 + H_2 = b$ , where  $b$  is given by Eq. (22). The line is parallel to the bisector of the second and fourth quadrants, and the point of tangency is simply given by  $H_1 = H_2 = b/2$ . The same reasoning can be extended to a multidimensional where  $N_f > 2$  case, and in this case, the point of tangency is given by  $H_1 = \dots = H_{N_f} = b/N_f$ .

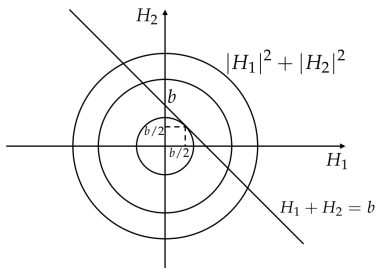


Figure 8. Geometrical interpretation of the minimization problem for  $N_f = 2$

It should be noted that the value  $b$  is what determine the minimum amount of ISI that the filter will induce. The smaller the value of  $b$ , the closer the point of tangency will be to the absolute minimum of the hyperparaboloid, i.e. the origin. With this in mind, it is reasonable to look for ways to minimize  $b$ . Considering Eq. (22), we can notice that minimising  $b$ , is equivalent to maximizing  $\sum_{H_i \in F_c} H_i$ . Since in general  $H_i$  are complex numbers, it follows that their sum will be maximized whenever they are all aligned, i.e. they have the same phase. Therefore this phase can be safely assumed to

be zero, therefore fixing  $H_i \in F_c$  to be real. Moreover, since the final ISI introduced by the filter will only depend on  $b$ , considering  $H_i \in F_f$  to be real is not a limiting factor.

We also checked this extremely simple closed solution to our optimization problem using general-purpose optimization software, obtaining exactly the same results.

## ACKNOWLEDGMENT

The authors would like to thank Maurizio Valvo, Stefano Capriata and their colleagues at Telecom Italia Lab (Turin, Italy) for the fruitful scientific discussion on the paper topics.

## REFERENCES

- [1] ITU-T, "40-Gigabit capable passive optical networks (NG-PON2)," *Recommendation G.989.1*.
- [2] R. Gaudino, V. Curri, and S. Capriata, "Propagation impairments due to Raman effect on the coexistence of GPON, XG-PON, RF-video and TWDM-PON," in *Optical Communication (ECOC 2013), 39th European Conference and Exhibition on*, Sept 2013, pp. 1–3.
- [3] G. Simon, F. SALIOU, P. Chanclou, B. L. Guyader, and L. Guillo, "Stimulated Raman Scattering Impairments Induced by NGPON2 Introduction in Co-existing PONs," in *Optical Fiber Communication Conference*. Optical Society of America, 2015, p. Th2A.52.
- [4] M. Cantono, V. Curri, A. Mecozzi, and R. Gaudino, "Interplay between Raman and polarization effects in next-generation passive optical networks," *Opt. Express*, vol. 23, no. 11, pp. 13 924–13 936, Jun 2015.
- [5] A. Shahpari, J. Reis, S. Ziaie, R. Ferreira, M. Lima, A. Pinto, and A. Teixeira, "Multi system next-generation PONs impact on video overlay," in *Optical Communication (ECOC 2013), 39th European Conference and Exhibition on*, Sept 2013, pp. 1–3.
- [6] F. Coppinger, L. Chen, and D. Piehler, "Nonlinear Raman cross-talk in a video overlay passive optical network," in *Optical Fiber Communications Conference, 2003. OFC 2003*, March 2003, pp. 285–286 vol.1.
- [7] M. Aviles, K. Litvin, J. Wang, B. Colella, F. Effenberger, and F. Tian, "Raman crosstalk in video overlay passive optical networks," in *Optical Fiber Communication Conference, 2004. OFC 2004*, vol. 2, Feb 2004, pp. 3 pp. vol.2–.
- [8] A. Tanaka, N. Cvijetic, and T. Wang, "Beyond 5dB nonlinear Raman crosstalk reduction via PSD control of 10Gb/s OOK in RF-video coexistence scenarios for next-generation PON," in *Optical Fiber Communication Conference*. Optical Society of America, 2014, p. M31.3.
- [9] J. Li, M. Bi, H. He, and W. Hu, "Suppression of SRS induced crosstalk in RF-video overlay TWDM-PON system using dicode coding," *Opt. Express*, vol. 22, no. 18, pp. 21 192–21 198, Sep 2014.
- [10] ITU, "J.186 - digital transmission of television signals – transmission equipment for multi-channel television signals over optical access networks by sub-carrier multiplexing (scm)," International Telecommunication Union, Series of Recommendations, 2002.
- [11] FCC, "Multichannel video and cable television service - technical standards," Federal Communications Commission, Standard, 1995.
- [12] C. Fludger, V. Handerek, and R. Mears, "Pump to signal RIN transfer in Raman fiber amplifiers," *Lightwave Technology, Journal of*, vol. 19, no. 8, pp. 1140–1148, Aug 2001.
- [13] R. H. Stolen, "Polarization effects in fiber Raman and Brillouin lasers," *Quantum Electronics, IEEE Journal of*, vol. 15, no. 10, pp. 1157–1160, Oct 1979.
- [14] D. Piehler, "Minimising nonlinear Raman crosstalk in future network overlays on legacy passive optical networks," *Electronics Letters*, vol. 50, no. 9, pp. 687–688, April 2014.
- [15] J. Proakis, *Digital Communications*, 4th ed. McGraw-Hill, Nov. 2000.
- [16] S. Mitra and S. Mitra, *Digital Signal Processing: A Computer-based Approach*. McGraw-Hill, 2011.